

Oxa Analogues of Nexturastat A Demonstrate Improved HDAC6 Selectivity and Superior Antileukaemia Activity

Marc Pflieger^{+, [a]}, Melf Sönnichsen^{+, [b]}, Nadine Horstick-Muche,^[a] Jing Yang,^[b, c] Julian Schliehe-Diecks,^[b] Andrea Schöler,^[d] Arndt Borkhardt,^[b] Alexandra Hamacher,^[a] Matthias U. Kassack,^[a] Finn K. Hansen,^[e] Sanil Bhatia,^{*, [b]} and Thomas Kurz^{*, [a]}

The acetylome is important for maintaining the homeostasis of cells. Abnormal changes can result in the pathogenesis of immunological or neurological diseases, and degeneration can promote the manifestation of cancer. In particular, pharmacological intervention in the acetylome with pan-histone deacetylase (HDAC) inhibitors is clinically validated. However, these drugs exhibit an undesirable risk-benefit profile due to severe side effects. Selective HDAC inhibitors might promote patient compliance and represent a valuable opportunity in personalised medicine. Therefore, we envisioned the development of

HDAC6-selective inhibitors. During our lead structure identification, we demonstrated that an alkoxyurea-based connecting unit proves to be beneficial for HDAC6 selectivity and established the synthesis of alkoxyurea-based hydroxamic acids. Herein, we report highly potent *N*-alkoxyurea-based hydroxamic acids with improved HDAC6 preference compared to nexturastat A. We further validated the biological activity of these oxa analogues of nexturastat A in a broad subset of leukaemia cell lines and demonstrated their superior anti-proliferative properties compared to nexturastat A.

Introduction

Histone deacetylases (HDACs) are proteases that catalyse the cleavage of acetylated lysine residues (isopeptide bonds).^[1] Human zinc dependant histone deacetylases (HDACs) are

classified into class I (HDAC1, HDAC2, HDAC3, HDAC8), class IIa (HDAC4, HDAC5, HDAC7, HDAC9), class IIb (HDAC6, HDAC10) and class IV (HDAC11). Depending on their cellular localisation, they influence the condensation state of histones,^[2] participate in the post-translational modifications of cytosolic proteins,^[3] or even might act as an epigenetic reader in the case of class IIa HDACs.^[4] Amongst humans, their diverse array of functions renders them a valuable target for the pharmacological intervention of immunological^[5–8] or neurodegenerative diseases^[9,10] and are clinically validated targets for the treatment of cancer.^[11]

Whilst CD1 has a high specificity in the substrate recognition of acetylated C-terminal lysine residues, CD2 exhibits a promiscuity towards a wide range of client proteins.^[12,13] In addition to those domains, HDAC6 displays an inherent zinc-finger ubiquitin binding domain (ZnF-UBP)^[13,14] that enables it to recognise ubiquitylated proteins. The rigidly controlled localisation of HDAC6 in the cytoplasm is the result of the interplay between the nuclear export signal (NES), the nuclear localisation signal (NLS) and the Ser–Glu-containing tetrapeptide (SE14).^[15]

HDAC6 catalyses the deacetylation of, for example, α -tubulin,^[16] cortactin^[17] and HSP90^[18] and is of relevance for the pathogenesis of cancer^[19] as well as in immunological^[20] and neurological diseases.^[21–23] Its participation in pathogenesis or disease progression is tissue dependant and of multifactorial nature. Despite intensive research, the clinical significance of HDAC6 selective inhibitors, as single agent, remains controversial.^[24] Increasing evidence suggest, that the anti-cancer effect of those biologically active compounds is the result of concentrations at which other HDAC isozymes, particularly class I HDACs, are also inhibited. Nevertheless, the pharmacological intervention of cancer by addressing HDAC6, remains a promising target due to its participation in the

[a] Dr. M. Pflieger,⁺ N. Horstick-Muche, Dr. A. Hamacher, Prof. Dr. M. U. Kassack, Prof. Dr. T. Kurz
 Institut für Pharmazeutische und Medizinische Chemie
 Heinrich-Heine-Universität Düsseldorf
 Universitätsstr. 1, 40225 Düsseldorf (Germany)
 E-mail: thomas.kurz@hhu.de


[b] M. Sönnichsen,⁺ J. Yang, J. Schliehe-Diecks, Prof. Dr. A. Borkhardt, Dr. S. Bhatia
 Department of Pediatric Oncology, Hematology and Clinical Immunology, Medical Faculty
 Heinrich Heine University Düsseldorf
 Universitätsstr. 1, 40225 Düsseldorf (Germany)
 E-mail: Sanil.Bhatia@med.uni-duesseldorf.de


[c] J. Yang
 Department of Medicine
 Yangzhou Polytechnic College
 West Wenchang Road 458, Yangzhou, 225009 (P.R. China)


[d] A. Schöler
 Institute for Drug Discovery, Medical Faculty
 Leipzig University
 Brüderstraße 34, 04103 Leipzig (Germany)

[e] Prof. Dr. F. K. Hansen
 Pharmaceutical and Cell Biological Chemistry, Pharmaceutical Institute
 University of Bonn
 An der Immenburg 4, 53121 Bonn (Germany)

[*] These authors contributed equally to this work.

 Supporting information for this article is available on the WWW under <https://doi.org/10.1002/cmdc.202001011>

 This article belongs to the joint Special Collection with ChemBioChem, "Chemical Epigenetics".

 © 2021 The Authors. ChemMedChem published by Wiley-VCH GmbH. This is an open access article under the terms of the Creative Commons Attribution Non-Commercial NoDerivs License, which permits use and distribution in any medium, provided the original work is properly cited, the use is non-commercial and no modifications or adaptations are made.

invasiveness of cancer cells and its immunomodulatory properties.

Currently approved HDAC inhibitors (HDACi) are vorinostat, belinostat, panobinostat, romidepsin for the treatment of haematological malignancies and tucidinostat (chidamide) for the treatment of breast cancer in China. All approved HDACi exhibit a mutual pharmacophore model: a zinc binding group (ZBG), a linker, and a cap group.^[25–27] Whilst romidepsin^[28,29] is preferential and tucidinostat^[30] selective for HDAC class I isozymes, the remaining are regarded as pan inhibitors as they do not differentiate between individual isozymes. Since the elucidation of structural information of HDACs,^[31] the design of selective inhibitors was significantly accelerated. Despite their high sequence identity inside the catalytic pocket, HDACs exhibit distinct features that allows a rational design for isozyme selective inhibitors. Particularly in comparison to HDAC1,^[32] HDAC6^[31] exhibits a much wider and shallower entrance tunnel (Figure 1).

Accumulating structural information of HDACs challenged the traditional HDACi pharmacophore model (ZBG, linker, cap) which was insufficient for the design of selective inhibitor and a revised pharmacophore model was developed. The pharmacophore model for HDAC6 inhibitors comprises of a ZBG, an aromatic linker and a sterically demanding surface cap group (S-CAP).^[33] Based on these structural features and the revised pharmacophore model, the selectivity towards HDAC6 can be governed by a sterically demanding cap group (Figure 2).

Two of the most prominent HDAC6 selective inhibitors are nexturastat A^[35,36] and tubastatin A,^[34] of which both exhibit a sterically demanding cap group. Whilst tubastatin A realises

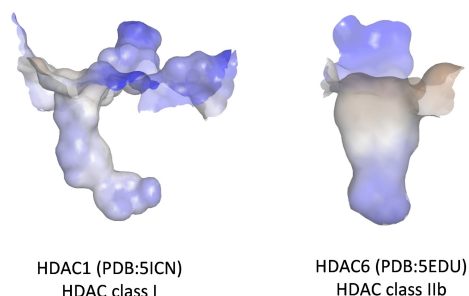


Figure 1. Surface comparison of HDAC1 and HDAC6.^[16,33]

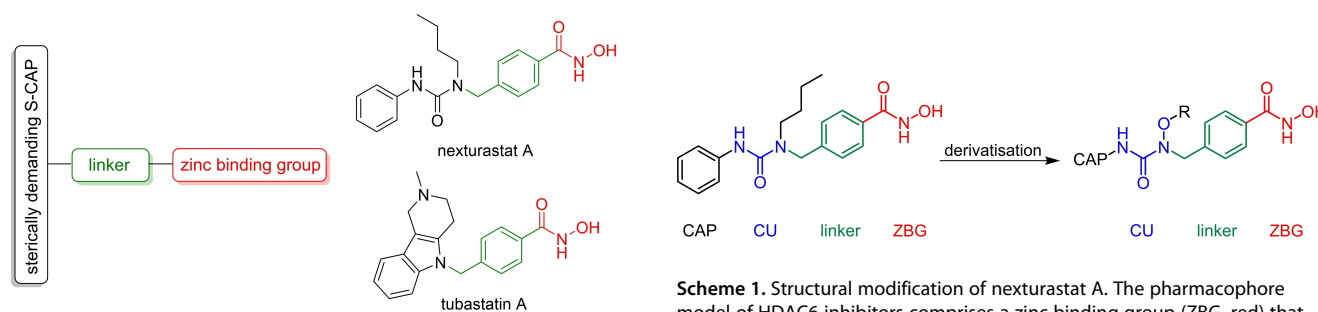


Figure 2. Revised pharmacophore model for the design of selective HDAC6 inhibitors.^[33–35]

this steric demand by a bulky cap group, nexturastat A facilitates its selectivity by the exhibition of a branched cap group.

Recently, we demonstrated that the modification of the functional group that connects the linker and the cap group of HDACi (connecting unit, CU) can significantly alter the isozyme profile of unselective HDACi (pan HDACi).^[37,38] The reported alkoxyamide and alkoxyurea derivatives of vorinostat and panobinostat exhibited a refined isozyme profile that resulted in a HDAC6 preference.

Here we report a rational derivatisation of Nexturastat A to improve HDAC6 selectivity (Scheme 1) and compounds with superior antiproliferative properties.

Results and Discussion

Nexturastat A is a selective HDAC6 inhibitor with a low-nanomolar activity and a reported 600-fold selectivity for HDAC6 over HDAC1.^[36] Despite its high selectivity reported^[36] by Bergman et al., nexturastat A exhibited only a selectivity index of 24 in our HDAC enzyme assays (Table 1). The lower selectivity, compared with the initial selectivity data, is in good agreement with recently published data by Vergani et al.^[39]

To increase the selectivity towards HDAC6, we envisioned structural modifications of nexturastat A by the introduction of an alkoxyurea-based connecting unit (CU), whilst maintaining the potency of nexturastat A.

Molecular docking

The focus of our rational design revolved around structural modifications of nexturastat A to establish a hydrogen bond interaction with Ser568 of the HDAC6 L1 loop segment. To support our initial hypothesis that alkoxyurea derivatives of nexturastat A could exhibit a hydrogen bond interaction with HDAC6, we have performed molecular docking studies with AutoDock 4.2 employing a previously validated docking protocol.^[38] Compound **4a** and nexturastat A were docked in HDAC6 (PDB ID: 5EDU).^[31] The molecular docking results suggest, that the CU of compound **4a** could rotate at the benzylic position to adapt a conformation to establish a

Scheme 1. Structural modification of nexturastat A. The pharmacophore model of HDAC6 inhibitors comprises a zinc binding group (ZBG, red) that coordinates to the zinc ion in the catalytic centre, a linker that interacts with the hydrophobic entrance tunnel and a sterically demanding cap group that is connected to the linker via the connecting group (CU).

Table 1. HDAC1-3/6/8 isozyme profiling of compounds **4 a** and **b**.

R'	R''	IC ₅₀ [μ M] HDAC1	HDAC2	HDAC3	HDAC6	HDAC8	SI ^{1/6}	SI ^{2/6}	SI ^{3/6}	SI ^{8/6}	
4a			0.742 \pm 0.039	1.42 \pm 0.082	0.902 \pm 0.008	0.020 \pm 0.003	4.64 \pm 0.84	37	71	45	232
4b			0.299 \pm 0.057	0.515 \pm 0.043	0.375 \pm 0.084	0.014 \pm 0.002	3.37 \pm 0.61	21	37	27	241
4c			0.715 \pm 0.010	1.14 \pm 0.074	0.972 \pm 0.064	0.022 \pm 0.002	4.46 \pm 0.41	33	52	44	203
4d			2.89 \pm 0.125	3.59 \pm 0.410	3.12 \pm 0.578	0.341 \pm 0.021	9.94 \pm 1.71	8.5	11	9.2	29.1
nexturastat A			0.504 \pm 0.033	0.861 \pm 0.008	0.730 \pm 0.033	0.021 \pm 0.001	9.91 \pm 1.25	24	41	35	472

Data are the mean \pm SD of at least two independent experiments, each carried out in duplicate wells.

hydrogen bonding interaction between Ser568 and the oxygen atom of the alkoxy side chain (Figure 3).

Synthesis of branched alkoxyurea based hydroxamic acids

In order to evaluate the influence of the alkoxyurea CU in respect to HDAC isozyme profile, the direct alkoxyurea derivative of Nexturastat A was synthesised (**4a**), based on our retrosynthetic analysis (Scheme 2).

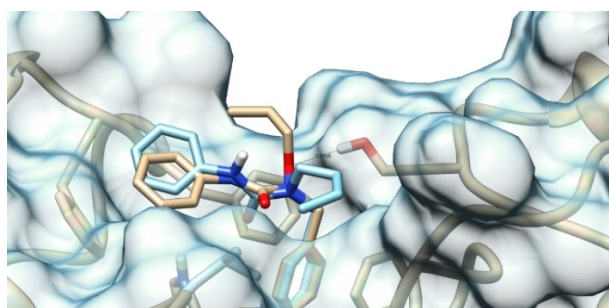
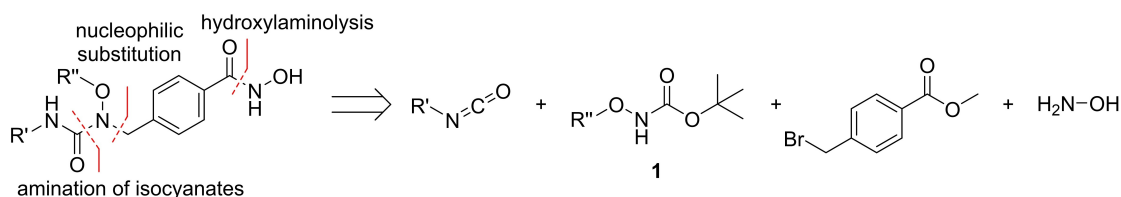


Figure 3. Proposed binding mode of compound **4a** (beige) and nexturastat A (cyan) in HDAC6 (PDB ID: 5EDU).



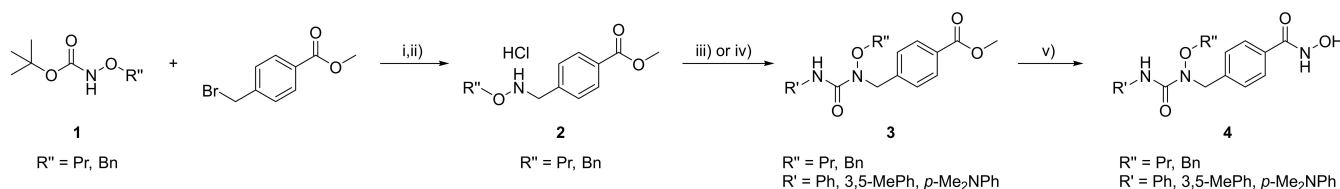
Scheme 2. Retrosynthetic analysis of alkoxyurea based hydroxamic acids.

N-Boc-*O*-alkylhydroxylamines (**1**) were synthesised either by *O*-alkylation of *N*-Boc-hydroxylamine with 1-bromopropane (**1a**) or by the *N*-Boc protection of *O*-benzyl hydroxylamine (**1b**).

The *O*-substituted hydroxylamine moiety was introduced to the benzyl linker by the *N*-alkylation of **1** with methyl 4-(bromomethyl)benzoate (Scheme 3). As the purification of this intermediate was laborious, **2** was accessed after Boc deprotection over two steps. Subsequently, the branched alkoxyurea derivatives **3a**, **3b**, **3d** were synthesised by the conversion of **2** with the respective isocyanate. In the case of **3c**, *N,N*-dimethyl-*p*-phenylenediamine was coupled with **2a** ($R'' = \text{Pr}$) by 4-nitrophenyl chloroformate. Finally, the esters were converted into the corresponding hydroxamic acids **4** by hydroxylaminolysis.

HDAC inhibition by branched alkoxyurea based hydroxamic acids

The branched alkoxyurea based hydroxamic acids **4** were subjected to HDAC1-3/6/8 isozyme profiling to evaluate their HDAC6 selectivity and their inhibitory potential. Table 1 depicts the isozyme profiling of compounds **4**. **4a** ($IC_{50} = 0.020 \pm 0.003 \mu\text{M}$), **4b** ($IC_{50} = 0.014 \pm 0.002 \mu\text{M}$) and **4c** ($IC_{50} = 0.022 \pm 0.002 \mu\text{M}$) demonstrated similar HDAC6 inhibition potencies to nexturastat A ($IC_{50} = 0.021 \pm 0.001$). A benzyl substituent (**4d**, $IC_{50} = 0.341 \pm 0.021 \mu\text{M}$) caused a significant loss in HDAC6



Scheme 3. Synthesis of branched alkoxyurea-based hydroxamic acids **4**. i) 1.10 equiv. methyl 4-(bromomethyl)benzoate 1.20 equiv. NaH; ii) 5.00 equiv. $\text{HCl}_{(\text{dioxane})}$, CH_2Cl_2 , 91–92% (2 steps) iii) 1.00 equiv. $\text{R}'\text{NCO}$, 1.00 equiv. DIPEA, CH_2Cl_2 , 73–85%, iv) 1.00 equiv. *N,N*-dimethyl-*p*-phenylenediamine, 1.00 equiv. 4-nitrophenyl chloroformate, 2.00 equiv. DIPEA; v) 30.0 equiv. $\text{H}_2\text{NOH}_{(\text{aq})}$, 10.0 equiv. NaOH, $\text{CH}_2\text{Cl}_2/\text{MeOH}$, 34% –76%.

inhibition, indicating that aliphatic substituents at R'' are beneficial for HDAC6 inhibition.

In contrast to the reported 600-fold selectivity of nexturastat A for HDAC6 over HDAC1, it showed a moderate selectivity index of 24 ($\text{SI}^{2/6} = 41$, $\text{SI}^{3/6} = 35$) in our enzyme assay. The hydroxylamine derivative **4a** showed a 1.5-, 1.7-, 1.3-fold higher $\text{SI}^{1/6}$, $\text{SI}^{2/6}$ and $\text{SI}^{3/6}$ than nexturastat A, respectively. A higher selectivity towards HDAC6 was anticipated by sterically demanding substituents such as 3,5-dimethylphenyl (**4b**) or by a 4-(*N,N*-dimethyl amino)-phenyl (**4c**). However, these substituent patterns had either no significant impact on the selectivity (**4c**) or was even disadvantageous in the case of **4b**. Furthermore, a benzyl substituent at R'' (**4d**) resulted in a significant decreased inhibition of HDAC6 ($0.341 \pm 0.021 \mu\text{M}$) with a concomitant decrease in selectivity as evidenced by the comparison with **4b**. Compound **4a–4c** demonstrated HDAC8 inhibition in the micromolar range ($3.37 \pm 0.61 \mu\text{M}$ to $4.64 \pm 0.84 \mu\text{M}$) and an approximately twofold lower $\text{SI}^{8/6}$ ($\text{SI}^{8/6}(\mathbf{4a}) = 232$, $\text{SI}^{8/6}(\mathbf{4c}) = 241$, $\text{SI}^{8/6}(\mathbf{4c}) = 203$) compared to nexturastat A ($\text{SI}^{8/6} = 472$). **4d**, exhibiting a benzyl substituent at R'' , showed highest HDAC8 inhibitory concentration ($\text{IC}_{50} = 9.94 \pm 1.71 \mu\text{M}$) and the lowest $\text{SI}^{8/6}$ ($\text{SI}^{8/6}(\mathbf{4d}) = 29.1$), which is mainly the result of a lower HDAC6 inhibition ($\text{IC}_{50} = 0.341 \pm 0.021 \mu\text{M}$).

Biological evaluation

To analyse the anti-cancer activity of the branched alkoxyurea based hydroxamic acids **4**, the *in vitro* antiproliferative efficacy of all four derivatives were tested on a broad range of leukaemia cell lines. The tested cell lines were HAL01, SUP-B15 (B-cell acute lymphoblastic leukaemia or B-ALL), K562 (chronic myeloid leukaemia or CML), Jurkat (T-cell acute lymphoblastic or T-ALL), HL60 and MOLM13 (acute myeloid leukaemia or AML). In the performed experiments, nexturastat A was used as a reference (Figure 4).

Compound **4b** showed the highest efficacy with the lowest IC_{50} (Figure 4, A) across all tested cell lines. In the AML cell lines HL60 and MOLM13, **4b** demonstrated IC_{50} values of $0.44 (\pm 0.024) \mu\text{M}$ and $0.11 (\pm 0.014) \mu\text{M}$, respectively. Against the other tested leukaemic entities, **4b** exhibited antiproliferative activities in the micromolar range from $1.6 (\pm 0.035) \mu\text{M}$ for K562 to $3.0 (\pm 0.14) \mu\text{M}$ for Jurkat.

The superior activity against the AML cell lines was a common feature shared by all four derivatives except for **4c**,

which showed a general weak efficacy against all cell lines compared to the other tested compounds. The weak antiproliferative properties of **4c** were surprising, as it exhibited a similar HDAC isozyme inhibition profile to the other inhibitors.

Similarly to nexturastat A, **4a** demonstrated the highest selectivity (antiproliferative profile) towards myeloid lineage originated leukaemic cell lines (K562, HL60 and MOLM13), amongst the tested alkoxyurea based hydroxamic acid derivatives, whereas **4b** exhibited pronounced antiproliferative activity across wide range of tested leukaemia cell lines. Compound **4** and nexturastat A were evaluated for their *in vitro* selectivity towards HDAC isoform (Figure 4B). HL60 (AML) cells were treated with **4** and nexturastat A in increasing concentrations, to compare the dose dependent hyperacetylation induction of α -tubulin and histone H3. The degree of α -tubulin hyperacetylation (HDAC6 inhibition marker) upon treatment with **4a** or **4d** was in agreement with the HDAC isozyme profile. Total α -tubulin was not affected by the treatment. However, nexturastat A and **4c** showed slightly higher levels of H3 acetylation compared to **4a** and **4b**. The total H3 was not affected by the treatment. Depetter et al. performed a comprehensive analysis of the biochemical and functional impact of selective HDAC6 inhibitors in a variety of *in vitro* and *in vivo* cancer models.^[24] HDAC6 inhibition results in α -tubulin acetylation but not in the anticipated anti-cancer effects. They have further demonstrated that selective HDAC6 inhibitor can result in a reduced cell growth as well as a reduced migratory and invasive activity at concentration, where other HDAC isozymes are co-inhibited. Based on these findings, the antiproliferative effect of selective HDACi is the result of the overall HDAC isozyme inhibition profile inside a cell.

The obtained data indicate, that **4b** exhibits a desirable isozyme inhibition profile that manifests in antiproliferative properties and therefore renders it a valuable hit for the development of active pharmaceutical ingredients for the treatment of a broad range of haematological malignancies.

Conclusion

HDAC6 is a major effector in the non-histone mediated regulation of cellular processes and represents a valuable target in the pharmacological intervention of immunological as well as neurological diseases. In addition, HDAC6 selective inhibitors remain valuable tools to explore the potential participation of

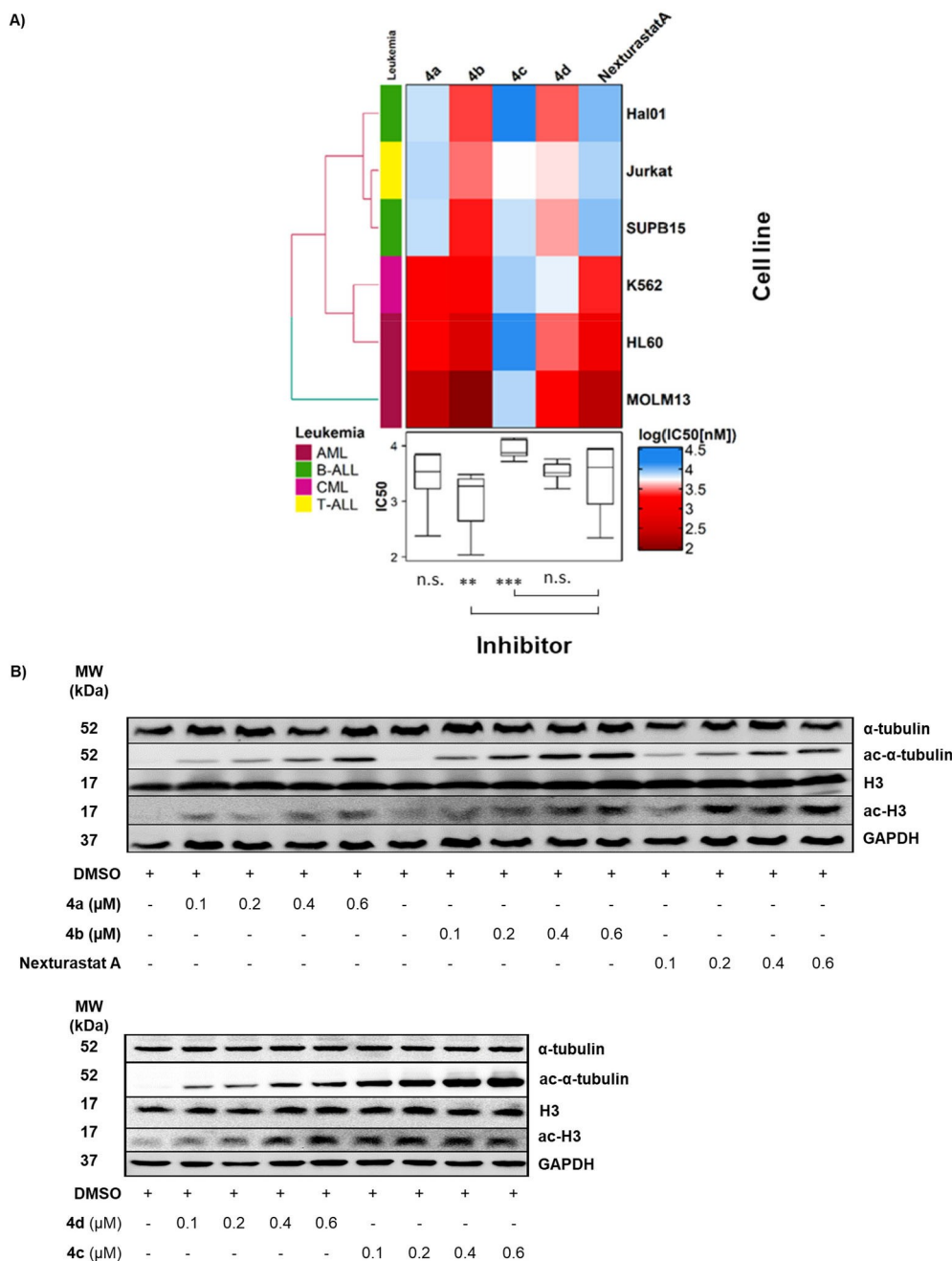


Figure 4. Cytotoxic and target specificity analysis. A) Comparative cellular viability ($\log IC_{50}$ [nM]) of different subgroups of leukaemic cell lines (HAL-01, Jurkat, SUP-B15, K562, HL60, MOLM13), after exposure to **4a**, **4b**, **4c** and **4d** in comparison to, nexturastat A ($n=3$). The IC_{50} data are plotted as a clustered heat map, followed by unsupervised hierarchical clustering. The vertical axis of the dendrogram exemplifies the dissimilarity between clusters, whereas the colour of the cell is related to its position along a $\log IC_{50}$ [nM] gradient. The boxplot shows the median IC_{50} ($\log IC_{50}$ [nM]) of the respective inhibitor across all tested leukaemic cell lines. The average IC_{50} values of each compound across all tested cell lines were used for statistical analysis. *, ** and n.s. indicate significant one-way ANOVA P values of < 0.05 , < 0.01 and > 0.05 , respectively. B) HL60 cells were treated with the indicated concentrations of **4a**, **4b**, **4c**, **4d** and nexturastat A for 24 h. Afterwards, cell lysates were immunoblotted with anti-acetyl- α -tubulin, acetyl-histone H3, total α -tubulin, and total histone H3 antibodies. GAPDH was used as a loading control.

HDAC6 in tumorigenesis. In this study, we developed a synthetic strategy for the synthesis of alkoxyurea based hydroxamic acids that exhibited an up to 1.5-fold higher $SI^{1/6}$ (**4a**) than the established HDAC6 selective inhibitor nexturastat A, whilst maintaining its potency. Amongst the tested inhibitors, **4b** was identified as the inhibitor with the most

pronounced antiproliferative activity across a selection of AML and non-AML cell lines that demonstrated an even higher antiproliferative activity than nexturastat A. In the tested cell lines, **4b** induced hyperacetylation of predominantly α -tubulin with superior antiproliferative activities compared to nexturastat A.

Acknowledgements

This work was funded by the Deutsche Forschungsgemeinschaft (DFG, German Research Foundation) 270650915 (Research Training Group GRK 2158). S.B. acknowledges financial support from the Forschungskommission (2018-04) and DSO-Netzwerkverbundes, HHU Düsseldorf. A.B. acknowledges financial support from the TransOnc priority program of German Cancer Aid through grant 70112951 (ENABLE). A.B. additionally acknowledges financial support from Löwenstern e.V. and from the Katharina Hardt Foundation. Open access funding enabled and organized by Projekt DEAL.

Conflict of Interest

The authors declare no conflict of interest.

Keywords: HDAC6 · HDAC isozyme profile · histone deacetylases · inhibitors · leukaemia

- [1] P. Bertrand, *Eur. J. Med. Chem.* **2010**, *45*, 2095–2116.
- [2] P. A. Marks, R. A. Rifkin, V. M. Richon, R. Breslow, T. Miller, W. K. Kelly, *Nat. Rev. Cancer* **2001**, *1*, 194–202.
- [3] P. Gallinari, S. Di Marco, P. Jones, M. Pallaoro, C. Steinkühler, *Cell Res.* **2007**, *17*, 195–211.
- [4] R. A. Mathias, A. J. Guise, I. M. Cristea, *Mol. Cell. Proteomics* **2015**, *14*, 456–470.
- [5] E. E. Hull, M. R. Montgomery, K. J. Leyva, *BioMed Res. Int.* **2016**, *2016*, 1–15.
- [6] P. V. Licciardi, T. C. Karagiannis, *ISRN Hematol.* **2012**, *2012*, 1–10.
- [7] O. Moreno-Gonzalo, M. Ramírez-Huesca, N. Blas-Rus, D. Cibrián, M. L. Saiz, I. Jorge, E. Camafeita, J. Vázquez, F. Sánchez-Madrid, *PLoS Pathog.* **2017**, *13*, e1006799.
- [8] T. Knox, E. Sahakian, D. Banik, M. Hadley, E. Palmer, S. Noonepalle, J. Kim, J. Powers, M. Gracia-Hernandez, V. Oliveira, et al., *Sci. Rep.* **2019**, *9*, 6136.
- [9] U. B. Pandey, Z. Nie, Y. Batlevi, B. A. McCray, G. P. Ritson, N. B. Nedelsky, S. L. Schwartz, N. A. Diprospero, M. A. Knight, O. Schuldiner, et al., *Nature* **2007**, *447*, 859–863.
- [10] C. Simões-Pires, V. Zwick, A. Nurisso, E. Schenker, P. A. Carrupt, M. Cuendet, *Mol. Neurodegener.* **2013**, *8*, 7.
- [11] P. G. Richardson, R. L. Schlossman, M. Alsina, D. M. Weber, S. E. Coutre, C. Gasparetto, S. Mukhopadhyay, M. S. Ondovik, M. Khan, C. S. Paley, et al., *Blood* **2013**, *122*, 2331–2337.
- [12] Y. Hai, D. W. Christianson, *Nat. Chem. Biol.* **2016**, *12*, 741–747.
- [13] Y. Miyake, J. J. Keusch, L. Wang, M. Saito, D. Hess, X. Wang, B. J. Melancon, P. Helquist, H. Gut, P. Matthias, *Nat. Chem. Biol.* **2016**, *12*, 748–754.
- [14] M. Haberland, R. L. Montgomery, E. N. Olson, *Nat. Rev. Genet.* **2009**, *10*, 32–42.
- [15] Y. Liu, L. Peng, E. Seto, S. Huang, Y. Qiu, *J. Biol. Chem.* **2012**, *287*, 29168–29174.
- [16] C. Hubbert, A. Guardiola, R. Shao, Y. Kawaguchi, A. Ito, A. Nixon, M. Yoshida, X. F. Wang, T. P. Yao, *Nature* **2002**, *417*, 455–458.
- [17] X. Zhang, Z. Yuan, Y. Zhang, S. Yong, A. Salas-Burgos, J. Koomen, N. Olashaw, J. T. Parsons, X. J. Yang, S. R. Dent, et al., *Mol. Cell* **2007**, *27*, 197–213.
- [18] J. J. Kovacs, P. J. M. Murphy, S. Gaillard, X. Zhao, J. T. Wu, C. V. Nicchitta, M. Yoshida, D. O. Toft, W. B. Pratt, T. P. Yao, *Mol. Cell* **2005**, *18*, 601–607.
- [19] T. Li, C. Zhang, S. Hassan, X. Liu, F. Song, K. Chen, W. Zhang, J. Yang, *J. Hematol. Oncol.* **2018**, *11*, 1–10.
- [20] A. Li, P. Chen, Y. Leng, J. Kang, *Oncogene* **2018**, *37*, 5952–5966.
- [21] M. Fukada, A. Nakayama, T. Mamiya, T. P. Yao, Y. Kawaguchi, *Neuropharmacology* **2016**, *110*, 470–479.
- [22] J. Jochems, J. Boulden, B. G. Lee, J. A. Blendy, M. Jarpe, R. Mazitschek, J. H. Van Duzer, S. Jones, O. Berton, *Neuropsychopharmacology* **2014**, *39*, 389–400.
- [23] N. Govindarajan, P. Rao, S. Burkhardt, F. Sananbenesi, O. M. Schlüter, F. Bradke, J. Lu, A. Fischer, *EMBO Mol. Med.* **2013**, *5*, 52–63.
- [24] Y. Depetter, S. Geurs, R. De Vreese, S. Goethals, E. Vandooorn, A. Laevens, J. Steenbrugge, E. Meyer, P. de Tullio, M. Bracke, et al., *Int. J. Cancer* **2019**, *145*, 735–747.
- [25] M. Jung, G. Brosch, D. Kölle, H. Scherf, C. Gerhäuser, P. Loidl, *J. Med. Chem.* **1999**, *42*, 4669–4679.
- [26] M. S. Finnin, J. R. Donigian, A. Cohen, V. M. Richon, R. A. Rifkin, P. A. Marks, R. Breslow, N. P. Pavletich, *Nature* **1999**, *401*, 188–193.
- [27] M. Jung, *Curr. Med. Chem.* **2012**, *8*, 1505–1511.
- [28] K. M. Vandermolen, W. McCulloch, C. J. Pearce, N. H. Oberlies, *J. Antibiot. (Tokyo)*. **2011**, *64*, 525–531.
- [29] S. P. Iyer, F. F. Foss, *Oncologist* **2015**, *20*, 1084–1091.
- [30] Y. K. Shi, M. Dong, X. Hong, W. Zhang, J. Feng, J. Zhu, L. Yu, X. Ke, H. Huang, Z. Shen, et al., *Ann. Oncol.* **2015**, *26*, 1766–1771.
- [31] Y. Hai, D. W. Christianson, *Nat. Chem. Biol.* **2016**, *12*, 741–747.
- [32] P. J. Watson, C. J. Millard, A. M. Riley, N. S. Robertson, L. C. Wright, H. Y. Godage, S. M. Cowley, A. G. Jamieson, B. V. L. Potter, J. W. R. Schwabe, *Nat. Commun.* **2016**, *7*, 11262.
- [33] J. Melesina, L. Praetorius, C. V. Simoben, D. Robaa, W. Sippl, *Future Med. Chem.* **2018**, *10*, 1537–1540.
- [34] K. V. Butler, J. Kalin, C. Brochier, G. Vistoli, B. Langley, A. P. Kozikowski, *J. Am. Chem. Soc.* **2010**, *132*, 10842–10846.
- [35] M. T. Tavares, S. Shen, T. Knox, M. Hadley, Z. Kutil, C. Bařinka, A. Villagra, A. P. Kozikowski, *ACS Med. Chem. Lett.* **2017**, *8*, 1031–1036.
- [36] J. A. Bergman, K. Woan, P. Perez-Villarroel, A. Villagra, E. M. Sotomayor, A. P. Kozikowski, *J. Med. Chem.* **2012**, *55*, 9891–9899.
- [37] M. Pflieger, A. Hamacher, T. Öz, N. Horstick-Muche, B. Boesen, C. Schrenk, M. U. Kassack, T. Kurz, *Bioorg. Med. Chem.* **2019**, *27*, 115036.
- [38] Y. Asfaha, C. Schrenk, L. A. Alves Avelar, F. Lange, C. Wang, J. J. Bandolik, A. Hamacher, M. U. Kassack, T. Kurz, *Bioorg. Med. Chem.* **2020**, *28*, 115108.
- [39] B. Vergani, G. Sandrone, M. Marchini, C. Ripamonti, E. Cellupica, E. Galbiati, G. Caprini, G. Pavich, G. Porro, I. Rocchio, et al., *J. Med. Chem.* **2019**, *62*, 10711–10739.

Manuscript received: December 31, 2020
Revised manuscript received: February 19, 2021
Accepted manuscript online: February 24, 2021
Version of record online: March 25, 2021